Optical band gap of cross-linked, curved, and radical polyaromatic hydrocarbons

Angiras Menon[a,d], Jochen A.H. Dreyer[a], Jacob W. Martin[a,d], Jethro Akroyd[a], John Robertson[b], Markus Kraft[a,c,d*]

[a] *Department of Chemical Engineering and Biotechnology, University of Cambridge, Philippa Fawcett Drive, Cambridge CB3 0AS, United Kingdom*

[b] *Department of Engineering, University of Cambridge, JJ Thomson Avenue,CB3 0FA Cambridge, United Kingdom*

[c] *Department of Chemical and Biomedical Engineering, Nanyang Technological University, 62 Nanyang Drive, 637459, Singapore* [d] *Cambridge Centre for Advanced Research and Education in Singapore (CARES), CREATE Tower, 1 Create Way, Singapore, 138602*

Supplementary Information

The structures of the 19 molecules whose OBG was measured experimentally by UV-Visible spectroscopy are are displayed in Fig. S1. Properties of these PAHs and the supplier are detailed in Table S1 below. The measured and calculated optical band gaps are also provided in Table S2. The calculated optical band gaps for naphthalene, biphenyl, and fluorene using a variety of hybrid functions are provided in Table S3.

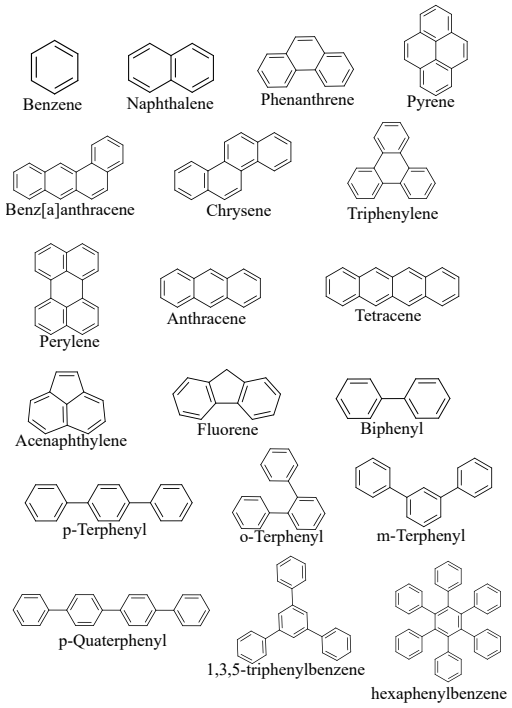

Figure S1: Structures of the 19 molecules studied both experimentally and computationally in the main paper.

Table S1: List of PAHs studied experimentally in this work and their properties.

Species	Number of Rings	$\frac{C}{H}$ ratio	Category	Supplier
Benzene	1	1.0	N/A	TCI
Naphthalene	2	1.25	Peri-Condensed/Acene	Sigma Aldrich
Phenanthrene	3	1.4	Peri-Condensed	Sigma Aldrich
Pyrene	4	1.6	Peri-Condensed	Sigma Aldrich
Benz[a]anthracene	4	1.5	Peri-Condensed	TCI
Chrysene	4	1.5	Peri-Condensed	TCI
Triphenylene	4	1.5	Peri-Condensed	Sigma Aldrich
Perylene	5	1.67	Peri-Condensed	TCI
Anthracene	3	1.4	Acene	Acros
Tetracene	4	1.5	Acene	Acros
Acenaphthylene	3(1 pentagonal)	1.5	Pentagonal	Sigma Aldrich
Fluorene	3(1 pentagonal)	1.3	Pentagonal	Sigma Aldrich
Biphenyl	2	1.2	Cross-linked	TCI
p-Terphenyl	3	1.29	Cross-linked	TCI
m-Terphenyl	3	1.29	Cross-linked	TCI
o-Terphenyl	3	1.29	Cross-linked	TCI
p-Quaterphenyl	4	1.33	Cross-linked	TCI
1,3,5-Triphenylbenzene	4	1.33	Cross-linked	Sigma Aldrich
Hexaphenylbenzene	6	1.4	Cross-linked	Sigma Aldrich

Table S2: Experimental and TD-DFT Band Gaps, HOMO energies, and LUMO energies in electron volts.

Species	$E_{g,\mathrm{Exp}}$	$E_{g,\mathrm{DFT}}$	E_{LUMO}	E_{HOMO}
Benzene	5.79	6.28	-0.64	-6.92
Naphthalene	4.22	4.31	-1.57	-5.88
Phenanthrene	4.16	4.02	-1.74	-5.76
Pyrene	3.64	3.42	-2.07	-5.49
Benz[a]anthracene	3.34	3.34	-2.08	-5.43
Chrysene	3.80	3.84	-1.79	-5.63
Triphenylene	4.10	4.43	-1.50	-5.93
Perylene	2.79	2.89	-2.53	-5.41
Anthracene	3.27	3.23	-2.11	-5.34
Tetracene	2.63	2.33	-2.68	-5.01
Acenaphthylene	3.59	3.68	-2.38	-6.06
Fluorene	4.06	4.33	-1.36	-5.68
Biphenyl	4.44	4.94	-1.20	-6.14
p-Terphenyl	4.00	4.32	-1.65	-5.97
m-Terphenyl	4.43	4.69	-1.46	-6.15
o-Terphenyl	4.21	4.68	-1.33	-6.01
p-Quaterphenyl	3.79	4.01	-1.81	-5.83
1,3,5-Triphenylbenzene	4.35	4.55	-1.50	-6.05
Hexaphenylbenzene	4.14	4.45	-1.58	-6.02

Table S3: HOMO-LUMO gaps of naphthalene, biphenyl, and Fluorene as computed by various different hybrid functionals, given in electron volts.

Functional	$E_{\mathrm{H-L,Naphthalene}}$	$E_{\mathrm{H-L,Biphenyl}}$	$E_{\mathrm{H-L,Fluorene}}$
HSE06	4.31	4.94	4.33
B3LYP	4.85	5.46	5.05
CAM-B3LYP	7.39	7.92	7.56
B971	4.94	5.44	5.13
PBE0	5.22	5.73	5.41
ω-B97xD	8.55	9.09	8.72
M06	5.26	5.76	5.44
B972	4.83	5.43	5.04

Determining Optical Band Gaps from UV/Visible Spectroscopy

We determine the optical band gap from UV/Visible spectroscopy using the absorption edge method as detailed in other works [1, 2, 3]. The peak of the low absorption band is located and then extrapolation is performed to locate the absorption edge, the point at which the absorption starts to occur, by finding the intersection between the baseline and the slope determined from the low absorption band maximum. This wavelength is then converted to the optical band gap using the standard formula:

$$E_g = \frac{1240}{\lambda_{\text{a.e}}}. \tag{1}$$

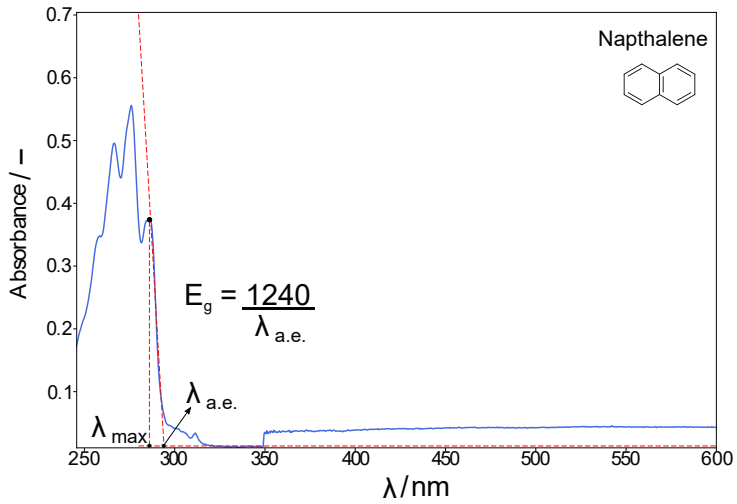

Figure S2: Example plot of absorbance against wavelength spectra for naphthalene zoomed in on the low energy absorption band. The method for determining the wavelength at the absorption edge is illustrated, along with the method of extrapolation.

The baseline value changes at 350 nm due to the change in light source from Visible to UV. The baseline value is taken as the baseline just before the absorption starts to occur. There is some noise present in the baseline prior to the start of the absorption, so an average is taken for the baseline value before absorption occurs.

Constrained Geometry Optimization of Corannulene

As mentioned in the main text, the curvature of corannulene was altered artificially by fixing the values of the internal dihedral angles between the pentagonal and the hexagonal planes in the molecule, as done in Martin et al [4]. This is illustrated in Fig S3 below:

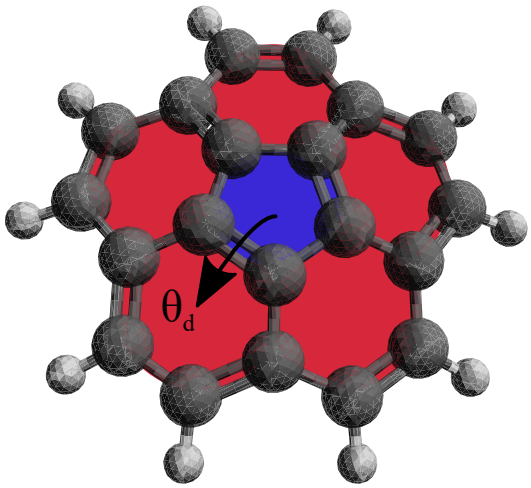

Figure S3: Top view of Corannulene molecule. The internal dihedral angles that are constrained during the geometry optimization are the angles between the pentagon (shaded in blue) and the hexagons (shaded in red).

The dihedral angle, θ_d, of corannulene from an unconstrained optimization using the B3LYP/6-311G** level of theory is 152.6°. θ_d was varied between 140°, representing a strained corannulene that is more curved than the normal conformer, and 180°, which represents a corannulene that has been restricted to be entirely planar.

Calculation of Aromatic Fluctuation Index

The aromatic fluctuation index (FLU) is defined in Matito et al. [5]. It is an aromatic index based on electron delocalization and has advantages over other commonly used aromaticity indices such as para-delocalization index (PDI) in that it can be applied to study non-6-membered rings as well. The FLU is calculated as follows:

$$\mathrm{FLU} = \frac{1}{n}\sum_{R}\left[\left(\frac{V(B)}{V(A)}\right)^{\mathrm{sgn}(V(B)-V(A))}\left(\frac{\delta(A,B)-\delta_{ref}(A,B)}{\delta_{ref}(A,B)}\right)\right]^2$$

$$R = \{A-B \mid A, B \text{ are neighbours in Ring-R}\}$$

The summation is taken over all adjacent pairs of carbon atoms, (A,B), when traversing the ring, R. V represents the valency of the atom, in question, δ is the delocalization of electrons for the C-C atom-pair, and δ_{ref} is the reference delocalization value as calculated for benzene,. A lower value of FLU therefore indicates a more aromatic ring. The calculations FLU for the rings in fluorene and acenaphthylene were performed using the Multiwfn program suite [6]. The FLU for the pentagonal ring in fluorene is 0.050 compared to 0.040 for acenaphthylene. This firstly suggests that the pentagon in acenaphthylene is more aromatic than the pentagon in fluorene, which would agree with their respective structures as the pentagon in fluorene is not fully delocalized. In

addition, these values of FLU for the pentagons would suggest low aromaticity of the five-membered ring in both fluorene and acenaphthylene. The FLU for the hexagonal rings in fluorene is 0.003 compared to 0.013 for the hexagonal rings in acenaphthylene. This suggests that the hexagonal rings in fluorene are more aromatic than those for acenaphthylene. In this case, the pentagonal rings in both molecules are not very aromatic. However, the hexagonal rings in fluorene are quite aromatic, and significantly more so than the hexagonal rings in acenaphthylene. This would suggest that fluorene is more aromatic than acenaphthylene, which could explain it having a significantly higher OBG.

Structures of PAHs studied

The molecular structures of the acenes and peri-condensed PAHs in Figures 3 and 9 are displayed in Figure S4. The molecular structures of the cross-linked PAHs in Figure 5 are displayed in Figure S5 and the curved PAHs in Figure 7 are displayed in Figure S6. The molecular structures of the various resonantly-stabilized-radical PAHs in Figure 10 are displayed in Figure S7.

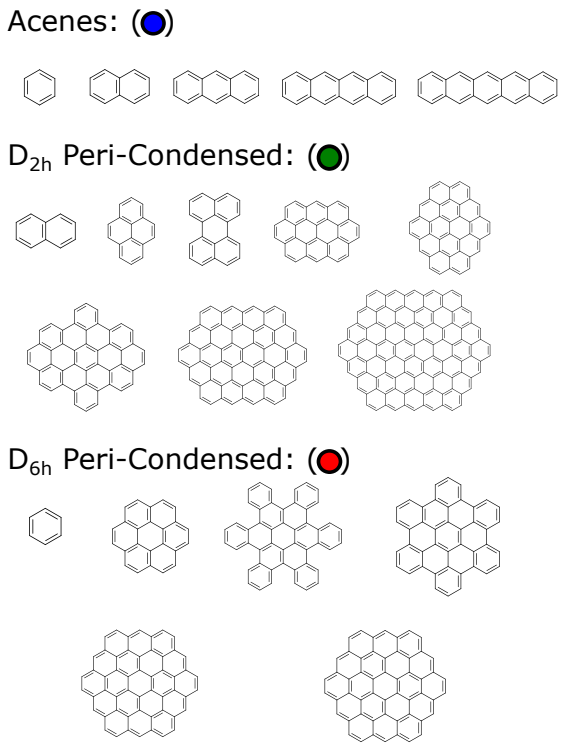

Figure S4: Molecular structures of the flat PAHs studied in this work, divided into acenes, D_{2h} PAHs, and D_{6h} PAHs.

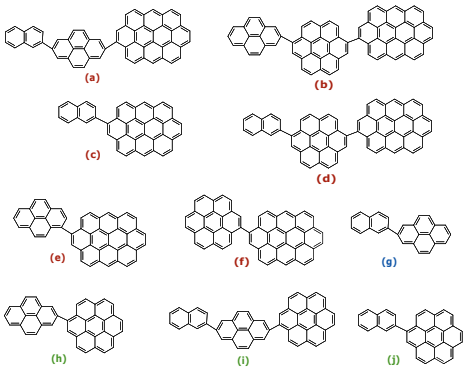

Figure S5: Molecular structures of the cross-linked PAHs consisting of different monomers studied in this work. Lettering and coloring matches with Figure 4a in the main article.

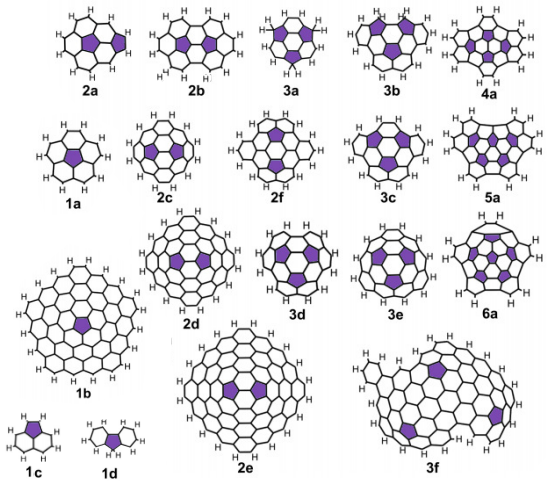

Figure S6: Molecular structures of the curved PAHs studied in this work. The number indicates the number of pentagons in the molecule and the lettering is to be consistent with [4]. Pentagons are shaded purple for clarity.

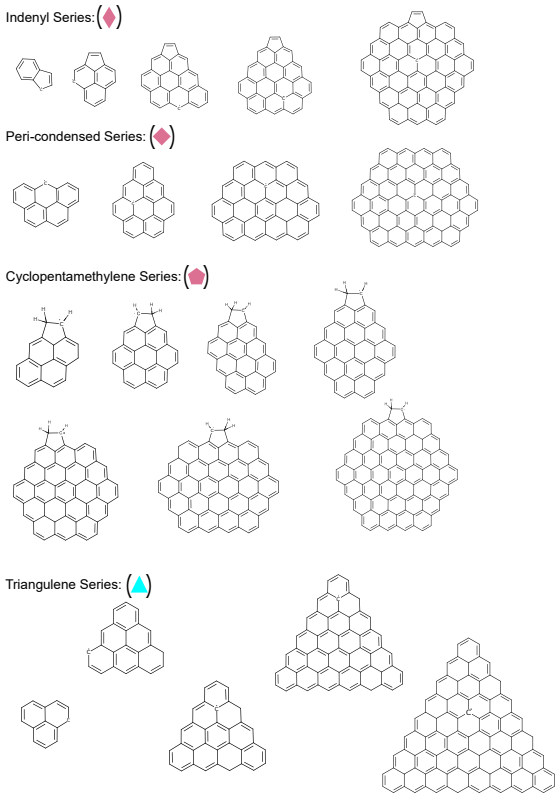

Figure S7: Molecular structures of the resonance-stabilized-radical PAHs studied in this work, categorized into the 4 main types.

Optimized Geometries

Optimized geometries of all of the PAHs studied in this work can be provided upon request.

References

[1] Y. Caglar, S. Ilican and M. Caglar, *Eur. Phys. J. B.*, 2007, **58**, 251–256.

[2] A. S. Bhadwal, R. M. Tripathi, R. K. Gupta, N. Kumar, R. P. Singh and A. Shrivastav, *RSC Adv.*, 2014, **4**, 9484–9490.

[3] J. C. Costa, R. J. Taveira, C. F. Lima, A. Mendes and L. M. Santos, *Opt. Mater.*, 2016, **58**, 51 – 60.

[4] J.W. Martin, R.I. Slavchov, E.K.Y Yapp, J. Akroyd, S. Mosbach, M. Kraft, *J. Phys. Chem. C.*, 2017, **0**, year.

[5] E. Matito, M. Duran and M. Sola, *J. Chem. Phys.*, 2005, **122**, 014109.

[6] T. Lu and F. Chen, *J. Comput. Chem.*, 2012, **33**, 580–592.